LUNAR ORBITAL REMOTE SENSING FOR ISRU – HELIUM-3 TEST CASE.

Carlton C. Allen NASA Johnson Space Center (retired); Co-I LRO Diviner Science Team
4 Spur Rd. Placitas, NM 87043 callen5126@comcast.net

Introduction: A striking number of spacecraft are being designed and built for landed missions to the Moon in the next decade. These include a mix of government and private missions to support both research and commerce, including the first steps toward lunar in-situ resource utilization (ISRU). Orbital remote sensing can provide a range of data vital to mission design and operation. This abstract describes a test case on the use of these datasets in support of a specific future mission devoted to helium-3, potentially a highly valuable lunar resource.

Orbital Datasets from Lunar Missions: Data from instruments on the Lunar Reconnaissance Orbiter (LRO) [1] and Clementine [2] missions cover nearly the entire lunar surface. These data include physical characteristics (surface slope, roughness, rock abundance, density and thermal parameters) which are key to spacecraft design and landing site selection. Additional orbital datasets include the abundances of specific elements and surface maturity. These datasets are well-calibrated and publicly accessible through the NASA Planetary Data System. They are also included in online geographic information systems, notable LROC Quikmap [3], which allow straightforward comparison.

Helium-3: The solar wind is dominated by hydrogen and the isotopes helium-4 and helium-3, which have been implanted into the lunar regolith over hundreds of millions of years. Experiments on Apollo samples demonstrate that over 90 % these gases can be released by vacuum heating [4]. Helium-3 release as high as 12 parts per billion (ppb; mass He / mass regolith) has been measured [5]. As discussed below, the yield of this isotope is correlated with the titanium content and maturity of specific regolith samples [6].

Helium-3 delivered to Earth has been recognized for decades as potentially the most valuable lunar resource [6]. Commercial interest in a gas present at the ppb level is motivated by the unique characteristics of helium-3 [7]. On Earth this rare isotope is used to reach temperatures near 0 K, which are essential for quantum computing. Helium-3 has important national security applications in detectors for smuggled nuclear material. The isotope is used in high-resolution medical imaging, particularly for pulmonary disease detection. A fusion reaction chain based on helium-3 holds the promise of energy production with minimal radioactivity. The current market price is approximately $19,000,000 / kg [7].

Test Case: The specific test case for orbital remote sensing in support of ISRU involves a lunar helium-3 mining and processing system [8,9]. This mission concept includes initial excavation of lunar regolith followed by heating to release implanted solar wind gases. The gases will then be cooled to near absolute zero in order to separate helium-3. This isotope is then packaged into vehicles for transport to Earth.

Region of Interest (ROI): A nearside mosaic of LROC Wide-Angle Camera (WAC) images [3] was overlaid with TiO_2 abundances derived from WAC multispectral data [10] using Quikmap. The highest TiO_2 nearside abundances are in Mare Tranquillitatis and Oceanus Procellarum. The Tranquillitatis area was chosen, based on its location near the well-characterized Apollo 11 landing site. A circular ROI with a diameter of 10 km was defined, centered at latitude 8.96 N and longitude 19.76 (Fig. 1). This location, in the area of highest TiO_2 concentration in the mare, is approximately 275 km northwest of the Apollo 11 site.

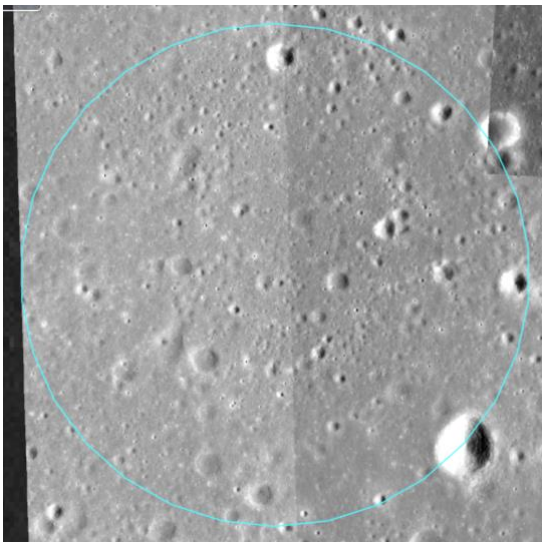

Figure 1. ROI 10 km diameter

Landing Safety: A mosaic of LRO Narrow-Angle Camera (NAC) images [3] shows many km-scale smooth areas within the ROI, along with a number of degraded sub-km craters. The autonomous landing precision of modern spacecraft is approximately 100 x 100 m [11], indicating that smooth areas can be successfully targeted.

Thermal data from the LRO Diviner radiometer is used to estimate the abundance of rocks on the lunar surface [12]. The mean rock abundance across the ROI is 0.008. This value is low compared to many areas on the Moon but is somewhat higher than the mean rock abundance of 0.005 for a 10 km diameter circle centered on the Apollo 11 site.

Surface roughness is derived from LRO Lunar Orbiter Laser Altimeter (LOLA) data [13]. The average roughness at 25 m across the ROI equals 0.40. The mean value for the Apollo 11 site is 0.39.

Surface slope is also derived from LOLA data [13]. The mean slope at 100 m for the ROI is 3.2 degrees. The mean value for the Apollo 11 site is 3.0 degrees.

The H-Parameter, related to regolith density and thermal conductivity, is derived from LRO Diviner data [14]. The mean H-Parameter value for the ROI is 0.07 m, while for the Apollo 11 site it is 0.08 m.

The soil temperature on the lunar surface can also be derived from LRO Diviner data [12]. The mean nighttime soil temperature within the ROI is 5.4 K. The equivalent value for the Apollo 11 landing site is 6.0 K.

Based on these orbital data, the surface landing hazards and thermal environments within the ROI are very similar to those encountered by the Apollo 11 astronauts. The autonomous system for the mission would need to be optimized to land safely within this ROI.

Helium-3 Yield: Solar wind helium-3 is preferentially concentrated in titanium-rich lunar regolith samples. The concentration of helium-3 increases with maturity, the duration of regolith exposure at the lunar surface [6].

The TiO_2 concentrations within the ROI are derived from WAC multispectral data [10]. The mean value is 10.4 wt. % with a standard deviation of 1.0 wt. % (Fig. 2). The comparable remote sensing value for a 10 km circle around the Apollo 11 site is 7.3 wt. % TiO_2 with a standard deviation of 0.9 wt. %. This concentration can be compared to the composition of Apollo 11 sample 10084, the largest regolith sample collected at any Apollo site. The bulk sample of 10084 has a TiO_2 concentration of 7.5 wt. % [15], close to the remote sensing value.

The unitless remote sensing parameter optical maturity (OMAT) is derived from UVVIS spectroscopic data [16] taken by the Clementine orbiter. The mean OMAT value for the ROI is 0.13, indicative of a mature regolith. The mean OMAT for a 10 km circle around the Apollo 11 site is also 0.13.

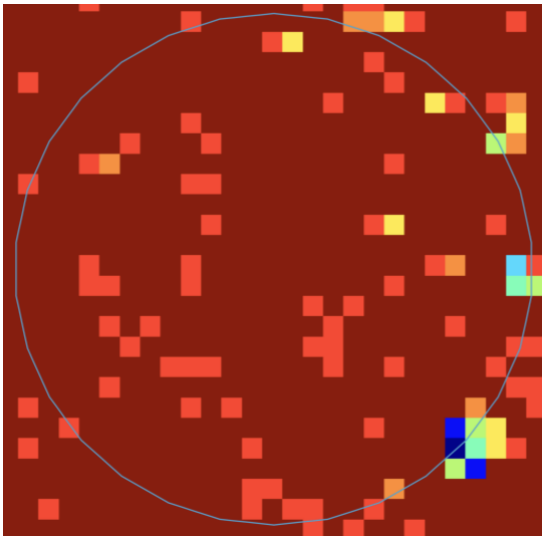

Figure 2. TiO_2 concentrations in the ROI

The mean helium-3 yield from heating two bulk aliquots of Apollo sample 84001 is 12 ppb [17]. The mean OMAT maturity values for the ROI and that of the 10 km circle around the Apollo 11 landing site are identical. Therefore, the helium-3 yield from the ROI is predicted to approximate the 10084 helium-3 yield times the ratio of TiO_2 concentrations for the two sites.

12 ppb x 10.4 wt. % / 7.3 wt. % = 17 ppb

The volume of regolith to be excavated scales directly with helium-3 yield. Assuming a regolith density of 1.6 g/cm^3, an excavation depth of 1 m and an end-to-end process efficiency of 100 %, one square kilometer within the ROI could produce 27.2 kg of helium-3. The ROI has an area of 78.5 km^2.

Excavating and processing regolith from the entire ROI could potentially produce approximately 2,135 kg of helium-3, with a market value of over 40 billion dollars.

References: [1] Tooley C. R. et al. (2010) *Space Sci. Rev., 150,* 23-62. [2] Nozette S. et al (1994) *Science, 266*, 1835-1839. [3] https://quickmap.lroc.im-ldi.com [4] Baur H. et al. (1972) LPSC III, 1947-1966. [5] Swindle T. D. et al. (1990) *UA/NASA Space. Engineering Research CenterTM-90/1.* [6] Johnson J. R. et al. (1999) *Geophys. Res. Lett., 26,* 385-388. [7] Bogaisky, J. (2025) *Forbes, Sept. 2.* [8] Frank, E. A. (2025) *LPSC 56th, Abs. 1185.* [9] Hoza K. et al. (2026) *LPSC 57th, Abs. 1370.* [10] Sato H. et al. (2017) *Icarus, 296,* 216-238. [11] Xin L. (2024) *Nature, 626,* 18-19. [12] Bandfield J. L. et al. (2011) *JGR, 116,* 18 pp. [13] Smith D. E. et al. (2017) *Icarus, 283,* 70-91. [14] Hayne P. O. et al. (2017) *JGR, 122,* 2371-2400. [15] Papike J. J. (1982) *Rev. Geophys. Space Phys., 20,* 761-826. [16] Lucey P. G. et al. (2000) *JGR, 105(E8),* 20377-20386. [17] Heymann D. and Yaniv A. (1970) *Proc. Apollo 11 Lunar Sci. Conf.,* 1247-1259.